Neurophysiology of Interceptive Behavior in the Primate: Encoding and Decoding Target Parameters in the Parietofrontal System

Hugo Merchant and Oswaldo Pérez

Abstract This chapter describes the encoding and decoding properties of target parameters in the primate parietofrontal system during an interception task of stimuli in real and apparent motion. The stimulus moved along a circular path with one of 5 speeds (180–540 degrees/s), and was intercepted at 6 o'clock by exerting a force pulse on a joystick that controlled a cursor on the screen. The real stimuli moved smoothly along the circular path, whereas in the apparent motion situation five stimuli were flashed successively at the vertices of a regular pentagon. First, we include a description of the neural responses associated with temporal and spatial aspects of the targets with real and apparent motion. Then, using a selected population of cells that encoded the target's angular position or time-to-contact, we tested the decoding power of the motor cortex and area 7a to reconstruct these variables in the real and apparent motion conditions. On the basis of these results, we suggest a possible neurophysiological mechanism involved in the integration of target information to trigger an interception movement.

Introduction

People and animals usually interact with objects in relative motion, that is, organisms are moving in the environment and/or objects are moving within the visual field toward or away from organisms. Thus, there are two main types of interactions between subjects and objects in relative motion: collision avoidance and the opposite, an interception. Successful control of these interactions is essential for survival. Fatal encounters can happen if the organism is not able to avoid collision or a predator, and a predator will eventually die if unable to catch its prey. This huge adaptative pressure suggests that the neural mechanisms underlying collision avoidance and interception have been sculpted by evolution throughout millions of years in different vertebrate and invertebrate species.

H. Merchant (✉)
Instituto de Neurobiología, UNAM, Campus Juriquilla, Querétaro Qro. 76230, México,
e-mail: merchant@inb.unam.mx

Although numerous studies have characterized different aspects of the interceptive behavior using an experimental psychology approach [26], few neurophysiological studies have determined the neural underpinnings of such an important action. However, recent findings from our group have provided the first clues regarding the neural mechanism of target interception [21–23, 30]. The present chapter focuses on the neurophysiological properties of the parietofrontal system in monkeys trained to intercept circularly moving targets in real or apparent motion. We describe the neural encoding and decoding abilities of the motor cortex and area 7a to represent different target attributes during this interception task.

Behavioral Aspects of an Interceptive Action

In manual hitting interceptions, the control of movement is done under explicit representations of where to go (the interception location or zone IZ) and how long it will take to get there (time-to-contact or TTC). Thus, in this type of behavior the time and position information are clearly distinguishable. Predictive and reactive models have formalized the integration of the temporal and spatial variables involved in the perceptual and motor components of manual hitting interceptions. In the predictive model, the interception movement is predetermined and is not influenced by visual information after the motor command is triggered. This model accounts for manual hitting interceptions with fast and ballistic movements and assumes that the programmed movement time is triggered after a key target parameter reaches a particular threshold. In some circumstances, it has been observed that the distance remaining to reach the interception zone (DTC_{tar}) can be a key parameter. In many others, the TTC_{tar} is the key parameter of preference [14, 34]. In contrast, the reactive strategy assumes that the interception movement starts at a target traveling time or distance, and then is further modulated in an ongoing fashion [8, 15]. Target pursuit is a behavior well explained by this model.

Summarizing the psychophysics of manual interception, a set of requirements must be satisfied to intercept a moving target. First, it is necessary to process the visual motion information of the target, including its actual position, TTC_{tar}, DTC_{tar}, and velocity. Second, the subject uses a predictive or reactive strategy to control the initiation of the interception movement, so that at the end of the movement the target is intercepted. Third, an interception movement should be implemented. This can be a ballistic movement with a predetermined direction and kinetics, or it can be a complex movement divided into submovements that can be regulated to optimize the precision of the interception. Finally, it is necessary to evaluate the end result of the interception, i.e., how precise it was. This information can be used to correct the strategy and the interception movement properties.

The neurophysiology of several of these behavioral components has been studied separately. It is well known that different cortical and subcortical areas, such as the middle temporal area (MT), process visual motion information. It has also been demonstrated that the different premotor areas and the primary motor cortex are involved in the preparation and execution of voluntary movements [13, 36]. Finally,

it has been suggested that different areas of the parietal and frontal lobes are engaged in visuomotor transformations [2]. Indeed, here we show how the visuomotor information is integrated in two areas of the parietofrontal system during an interception task [25]. Initially, however, we describe the cortical network engaged in visual motion processing.

Visual Motion Processing

Visual motion is a powerful stimulus for activating a large portion of the cerebral cortex. Neurophysiological studies in monkeys [1, 28] and functional neuroimaging studies in human subjects [5, 38] have documented the involvement of several areas in stimulus motion processing, including the MT [37], medial superior temporal area (MST) [35], superior temporal polysensory area [4], area 7a [18, 27, 33], and the ventral intraparietal area [6]. More detailed analyses of the neural mechanisms underlying visual motion processing have been performed in monkey experiments, the results of which indicate that different areas relate to different aspects of this processing. The direction of rectilinear motion is explicitly represented in the neural activity of the MT, a structure that projects to the MST, areas 7a and 7m, and VIP. These target areas are part of the posterior parietal cortex (PPC). Cells in the MST and area 7a not only respond to rectilinear motion, but also to optic flow stimuli, including stimulus motion in depth [9, 18, 33]. Neurons in the MST are tuned to the focus of expansion and can code for the direction of heading [3, 10]. The responses of area 7a neurons to optic flow stimuli appear to be more complex than those in the MST, since individual neurons respond similarly to opposed directions of motion, like clockwise (CW) and counterclockwise (CCW) rotations, upward and downward motions, or rightward and leftward translations [19]. Interestingly, optical expansion is the most prominent stimulus driving the activity of neurons in this area. Thus, the PPC can process optic flow information in a very complex fashion. It is reasonable to expect, then, that the PPC is a good candidate for the neural representation of TTC in primates. In fact, our group was the first to characterize the neural correlates of TTC_{tar} in area 7a and the motor cortex in the monkey [22]. Furthermore, in a recent fMRI study, it was demonstrated that the parietofrontal system in humans is specifically activated during perception of TTC judgments [12]. Besides the representation of TTC and direction of motion, areas such as the MT, MST, and area 7a also code for the speed of visual motion [11, 17, 29].

Overall, the current knowledge of visual motion processing indicates that the motor system has access to TTC_{tar}, DTC_{tar}, and target velocity to drive the interceptive response. This visual information travels to premotor areas and then to the primary motor cortex from different areas of the PPC. Therefore, the anatomic evidence indicates that the neural substrate of interceptive actions may be a distributed network engaging the parietofrontal system. In the following sections, we review some neural correlates of target interception in two important nodes of the parietofrontal system: area 7a and the motor cortex. We begin by describing the interception task used in these studies.

The Interception Task

The task required the interception of a moving target at 6 o'clock in its circular trajectory by applying a downward force pulse on a pseudoisometric joystick that controlled a cursor on the computer monitor (Fig. 1a) [20]. The target moved CCW with one of five speeds, ranging from 180 to 540 degrees/s. In addition to the real motion condition where the targets moved smoothly along a low contrast circular path, we also used an apparent motion situation where the target was flashed successively at the vertices of a regular pentagon [32]. In the latter condition, an illusion of a stimulus continuously moving along the circular path was obtained at target speeds above ∼315 degrees/s in human subjects [24]. We included path-guided apparent motion because we were interested in comparing the behavioral strategy and the overall neural mechanisms during the interception of stimuli with real and apparent motion. The hypothesis here was that the neural underpinnings of target interception is different during real and apparent motion conditions.

   In this task the monkeys used a predictive strategy for interception, producing predetermined ballistic movements. We, therefore, could investigate the possible key parameter used to control the initiation of the interception movement. For that purpose, we calculated TTC_{tar} and DTC_{tar} at the beginning of the effector movement. We found that DTC_{tar} increased asymptotically as a function of the stimulus speed in both motion conditions (Fig. 1b, *top*). In addition, the movement time (which corresponded to TTC_{tar} in these conditions) decreased slightly as a function of the stimulus speed, and it was larger in the real than in the apparent motion condition (Fig. 1b, *bottom*). Despite these results it was difficult to unambiguously identify the key parameter used for interception. Nevertheless, as we will show later, the neurophysiological data collected in the parietofrontal system suggest that TTC_{tar} is used to trigger the interception movement in both the real and apparent motion conditions [22].

Sensorimotor Processing During the Interception
of Circularly Moving Targets

In a previous study, we determined quantitatively the relation between the temporal pattern of neural activation and different aspects of the target and the motor execution during the interception task [22]. We designed a general multiple linear regression model to test the effects of different parameters on the time-varying neural activity. These parameters were the direction cosines of the stimulus angle, TTC_{tar}, the vertical hand force, and the vertical hand force velocity. This analysis revealed that the time-varying neuronal activity in area 7a and in the motor cortex was related to various aspects of stimulus motion and hand force in conditions of both the real and apparent motion, with stimulus-related activity prevailing in area 7a and hand-related activity prevailing in the motor cortex (Fig. 2). The most important
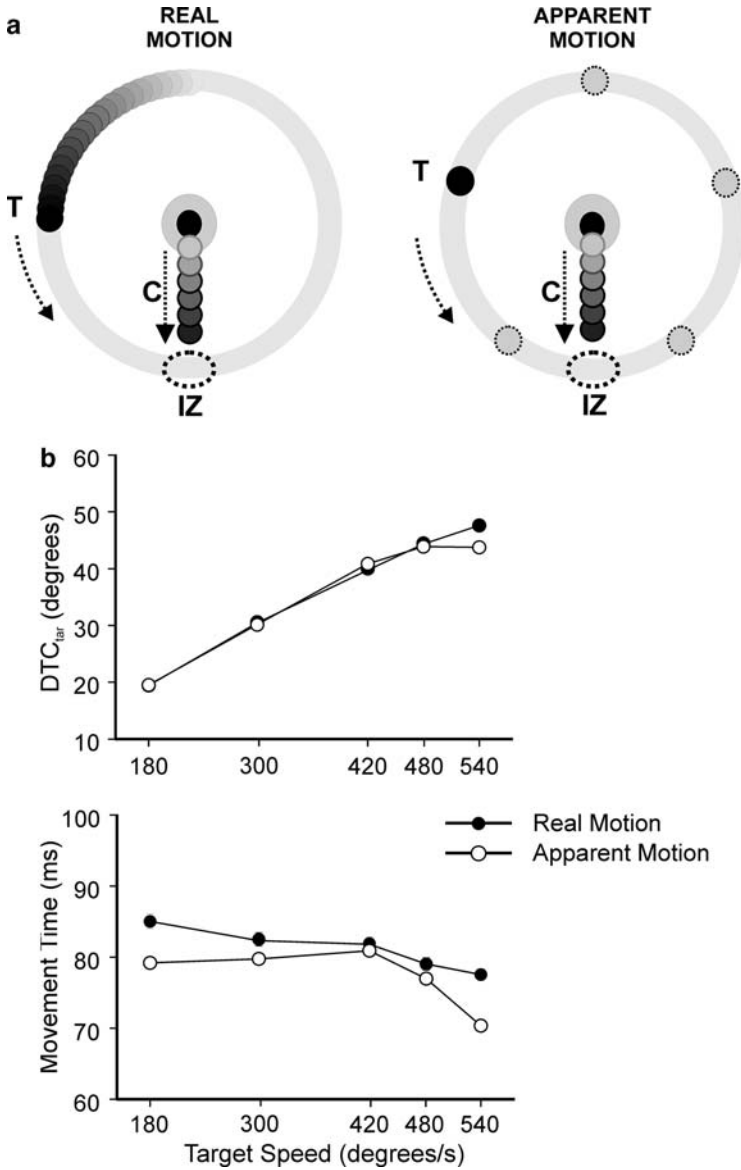
Fig. 1 (**a**) Interception task of circularly moving targets. T represents the smoothly moving target in the real motion condition, or the flashing stimulus at the vertices of a regular pentagon in the apparent motion condition; *C* cursor, *IZ* interception zone. (**b**) Behavioral performance during the interception task. *Top*, target distance to contact (DTC$_{tar}$) at the beginning of the interception movement; *bottom*, movement time is plotted as a function of the stimulus speed. *Filled circles* correspond to the real motion and *open circles* to the apparent motion condition. Modified from [20]
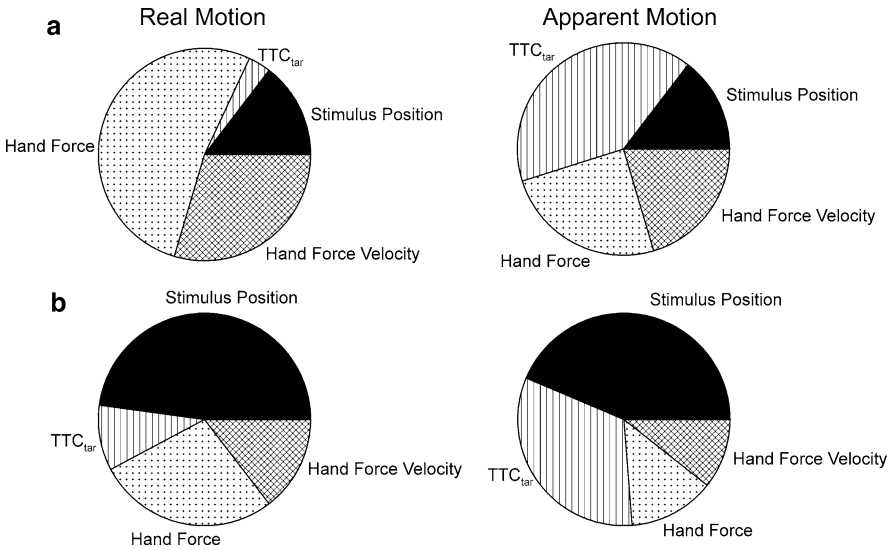
Fig. 2 Percentages of neurons in the real and apparent motion conditions, for which the noted parameter was ranked first using the standardized coefficients obtained from the multiple regression analysis. (**a**) Motor cortex. (**b**) Area 7a. Modified from [22]

finding was that the neural activity was selectively associated with the stimulus angle during real motion, whereas it was tightly correlated with TTC_{tar} in the apparent motion condition, particularly in the motor cortex (Fig. 2).

Encoding of Angular Position and Time-to-Contact During the Interception Task

As a following step, we compared how the time-varying neural activity was specifically related to the stimulus angle or the TTC_{tar}, in both motor cortex and area 7a. Independent linear regression models were carried out to test which target parameter was better explained by the temporal profile of activation for each target speed, in both the real and apparent motion conditions. The first model was defined as:

$$f_{t+\Delta} = b_0 + b_1 \cos \theta_t + b_2 \sin \theta_t + \varepsilon_t, \qquad (1)$$

where f_t is the mean spike density function at time t (20 ms window), Δ was the time lag between the neural activity and the independent variables and varied from -160 to $+160$ ms, b_0 is a constant, b_1 and b_2 are the regression coefficients for the stimulus angle (also referred to as θ or theta), and ε_t is the error. The second model was defined as:

$$f_{t+\Delta} = b_0 + b_1 \tau_t + \varepsilon_t \qquad (2)$$

with the same parameter definitions as (1), except that here b_1 is the regression coefficient for TTC_{tar} (also referred to as τ).

The adjusted R^2 was used to compare the goodness of fit, and the model with the highest value (1) vs. (2) was used for further analysis if the winning regression ANOVA was significant ($p < 0.05$). A total of 587 neurons in the motor cortex and 458 neurons in area 7a were analyzed using the two models, since these cells showed significant effects in the multiple linear regression model described earlier [22]. These analyses revealed again that the time-varying neuronal activity in area 7a and the motor cortex was related to different aspects of the target motion in both the real and apparent motion conditions. Neurons in area 7a showed that the target angle was the best parameter to explain the time-varying neural activity in both motion conditions (Table 1). In contrast, in the motor cortex the neural activity was selectively associated with the TTC_{tar}, in both the real and the apparent motion (Table 2).

Table 1 Percent and total number of neurons in area 7a that showed significant regression models from (1) or (2) and where the target angular position (θ) or the time-to-contact (TTC_{tar}) was the best parameter to explain the temporal profile of activation

Motion condition	Target velocity	% theta	% TTC_{tar}	Total neurons
Real Motion	180	70.85	29.15	247
	300	73.21	26.79	265
	420	74.45	25.55	227
	480	73.68	26.32	209
	540	73.14	26.86	175
Apparent motion	180	83.33	16.67	396
	300	79.40	20.60	369
	420	69.00	31.00	400
	480	69.04	30.96	394
	540	75.34	24.66	373

Table 2 Percent and total number of motor cortical cells that showed significant regression models from (1) or (2) and where the target angular position (θ) or the time-to-contact (TTC_{tar}) was the best parameter to explain the temporal profile of activation

Motion condition	Target velocity	% Theta	% TTC_{tar}	Total neurons
Real motion	180	27.00	73.00	337
	300	23.12	76.88	346
	420	24.41	75.59	299
	480	26.92	73.08	312
	540	22.97	77.03	296
Apparent motion	180	16.37	83.63	452
	300	21.70	78.30	447
	420	24.46	75.54	462
	480	27.20	72.80	478
	540	18.92	81.08	465
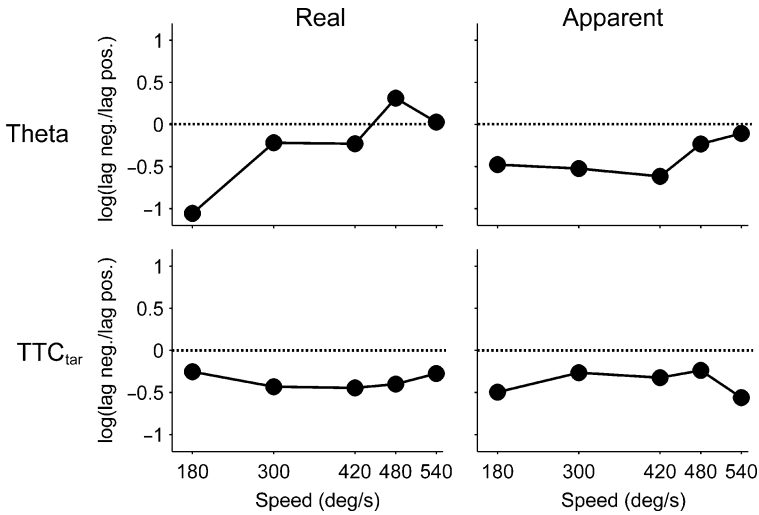
Fig. 3 The logarithm of the quotient between positive and negative lags plotted against the target speed for significant regressions in (1) (*Theta*, *top*) or (2) (TTC$_{tar}$, *bottom*) for the real (*right*) and apparent (*left*) motion conditions in the motor cortex

A different question concerns the time shifts of the stimulus angle and TTC for which the highest adjusted R^2 values were obtained across cells, target speeds, and motion conditions. Since the neural activity was shifted with respect to the independent variables: a negative shift indicated that the neural activity was leading the variable (predictive response), whereas a positive shift indicated that the variable was leading the neural activity (sensory response). In the motor cortex, the neural time shift distributions were skewed toward the predictive side. The overall median of the distribution of lags for all target speeds was -20 ms for both real and apparent motion conditions. To further analyze the time shifts for the best regression models in (1) and (2), we plotted the logarithm of the quotient (log-ratio) between all positive and all negative lags against the target speed (Fig. 3). In the apparent motion condition, both the target angle (θ) and TTC$_{tar}$ showed negative log-ratio values, indicating that the best time shifts were predictive across the target speeds. The same was observed for the TTC$_{tar}$ in the real motion condition; however, the target angle showed positive log-ratio values at the highest target speeds in this motion condition. Nevertheless, no significant differences between the lag distributions in the real and apparent motion conditions were observed for target angle or TTC$_{tar}$ (Kolmogorov–Smirnov test, $p > 0.05$). Therefore, these findings suggest that the time-varying activity of the motor cortex can encode the TTC$_{tar}$ and the target angle in a predictive fashion in both motion conditions.

In area 7a the neural time shift distributions for the highest adjusted R^2 models were skewed toward positive values (medians: 40 ms apparent, 20 ms real motion condition), indicating that area 7a neurons were responding to the change in the
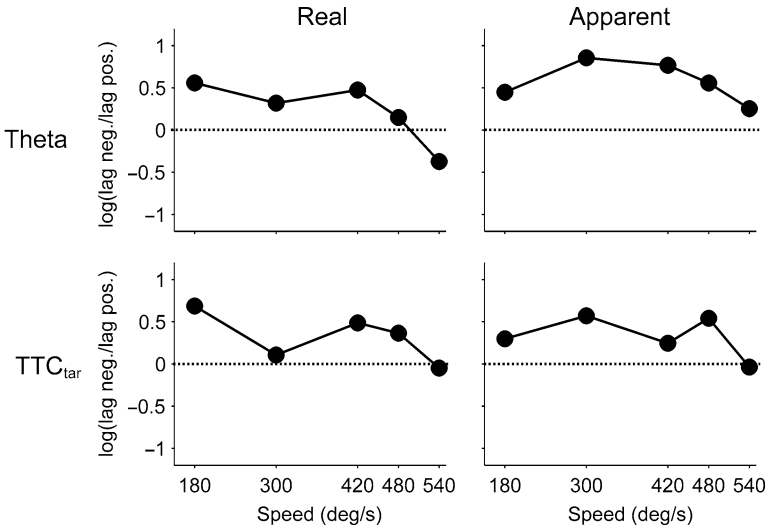
Fig. 4 The logarithm of the quotient between positive and negative lags plotted against the target speed for significant regressions in (1) (Theta, *top*) or (2) (TTC$_{tar}$, *bottom*) for the conditions of real (*right*) and apparent (*left*) motion in area 7a

target angle and TTC$_{tar}$. Actually, the log-ratio values were positive for most motion conditions and target speeds, with the exception of the target angle at the highest target speed, which showed a negative value, and hence predictive responses, in the real motion condition (Fig. 4). However, again, no significant differences were found between the target angle or the TTC$_{tar}$ lag distributions in the real and apparent motion conditions in this parietal area (Kolmogorov–Smirnov test, $p > 0.05$). Overall, these results emphasize the sensory role of area 7a in visual motion processing, with an initial reconstruction of the target TTC for real and apparent moving targets that could be transferred to the frontal areas for further processing.

As a final point, it is important to mention that the results of regressions from (1) and (2) were not totally consistent with the multiple regression analysis of the previous section. Specifically, during the real motion condition more neurons showed better fittings for the target angle in the previous analysis, whereas for (1) and (2), TTC$_{tar}$ was the best explanatory parameter in both areas. The most probable cause for this discrepancy is the fact that in the previous multiple regression model, we included the hand force and hand force velocity, which have some degree of collinearity with the TTC$_{tar}$. Therefore, the discrepancy probably reflects a competition between TTC$_{tar}$ and the arm movement parameters in the regression model of (2), competition that is quite relevant in the motor cortical cell activity. Then, to explore whether the activity of both areas carried enough information regarding the target angle and the TTC$_{tar}$, in the following section, we performed a detailed decoding analysis on these parameters.

Decoding of Angular Position and Tau During Interception of Circularly Moving Targets

Once we had determined the dependence of the neural responses on the target angle or TTC_{tar}, we used a Bayesian analysis approach to directly address the inverse problem: given the firing rates of these cells, how can we infer the spatial and temporal parameters of the target. The basic method assumes that we know the encoding functions $f_1(x), f_2(x), \ldots, f_N(x)$ associated with the time series for the target parameter (angle or TTC_{tar}) of a population of N cells from (1) or (2). Given the number of spikes fired by the cells within a time interval from $T - \Delta/2$ to $T + \Delta/2$, where Δ is the length of the time window (20 ms), the goal is to compute the probability distribution of the target angle or TTC_{tar} at time T. Notice that what is to be computed here is a distribution of the target parameter, not a single value. Thus, we always can take the most probable value, which corresponds to the peak of the probability distribution, as the most likely reconstructed target angle or TTC_{tar}.

Let the vector $\mathbf{x}$ be the target parameter, and the vector $n = (n_1, n_2, \ldots, n_N)$ be the numbers of spikes fired by our recorded cells within the time window t, where n_i is the number of spikes of cell i. The reconstruction is based on the standard Bayes formula of conditional probability:

$$P(x|n) = \frac{P(n|x) p(n)}{P(r)}. \tag{3}$$

The goal is to compute $P(\mathbf{x}|\mathbf{n})$, that is the probability for the target parameter to be at the value $\mathbf{x}$, given the number of spikes $\mathbf{n}$. $P(\mathbf{x})$ is the probability for the target to be at a particular value $\mathbf{x}$, which was fixed during the experiment. The probability $P(\mathbf{n})$ for the occurrence of the number of spikes $\mathbf{n}$ is equal to the mean of the conditional probability $P(\mathbf{n}|\mathbf{x})$ since $\mathbf{x}$ is deterministic in this experiment. Therefore, $P(\mathbf{n})$ is fixed and does not have to be estimated directly. Consequently, given that $P(\mathbf{n})$ and $P(\mathbf{x})$ are constant in this experiment then $P(\mathbf{x}|\mathbf{n})$ is a constant multiple of $P(\mathbf{n}|\mathbf{x})$.

Thus, the key step is to evaluate $P(\mathbf{n}|\mathbf{x})$, which is the probability for the numbers of spikes $\mathbf{n}$ to occur, given that we know the target parameter $\mathbf{x}$. It is intuitively clear that this probability is determined by the estimated firing rates from (1) or (2). More precisely, if we assume that the spikes have a Poisson distribution and that different cells are statistically independent of one another, then we can obtain the explicit expression:

$$P(n|x) = \prod_{i=1}^{N} \frac{(f_i(x)T)^{n_i}}{n_i!} e^{-f_i(x)T}, \tag{4}$$

where $f_i(x)$ is the average predicted firing rate of cell i of a population of N cells, $\mathbf{x}$ is the target parameter, and T is the length of the time window.

The Bayesian reconstruction method uses (4) to compute the probability $P(\mathbf{n}|\mathbf{x})$ for the target parameter to be at the value $\mathbf{x}$, given the numbers of spikes $\mathbf{n}$ of all the cells within the time window. In this probability distribution, the peak value is taken as the magnitude of the reconstructed target parameter. In other words:

$$\hat{x}\text{Bayes} = \arg\max_{x} P \langle n|x \rangle.$$
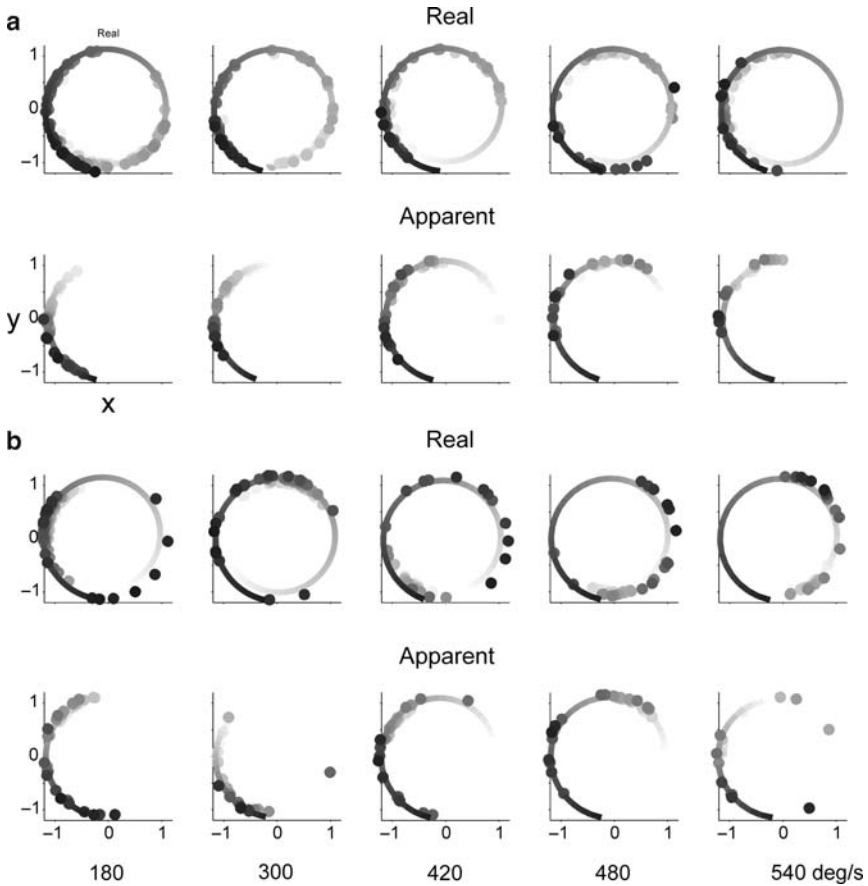
Fig. 5 Mean predicted angular position over time using ensembles of 50 neurons during the real and apparent motion conditions and for the five different stimulus speeds. (**a**) Area 7a. (**b**) Motor cortex. The real (*line*) and predicted (*circles*) positions are color coded in a gray scale, starting at time zero (target onset) in light gray, and ending in black at the last time bin (interception time)

By sliding the time window forward, the entire trajectory of the target parameter can be reconstructed from the time-varying activity in the neural population.

To systematically decode both target parameters, we used the cells with significant regressions from (1) or (2). However, since the number of significant cells varied across motion conditions, target speeds, and cortical areas, we used a constant population of 50 cells to decode both target parameters across all these conditions, to avoid a population-size effect in the reconstructed angular position or TTC_{tar}. In fact, we carried out 100 decodifications for each condition using permuted populations of 50 cells (from the total number of neurons) and cross-validation (across trials) with the purpose of sampling the reconstruction accuracy (variance and bias, see eqs. 3.38 and 3.39 of [7]) within the overall cell population.
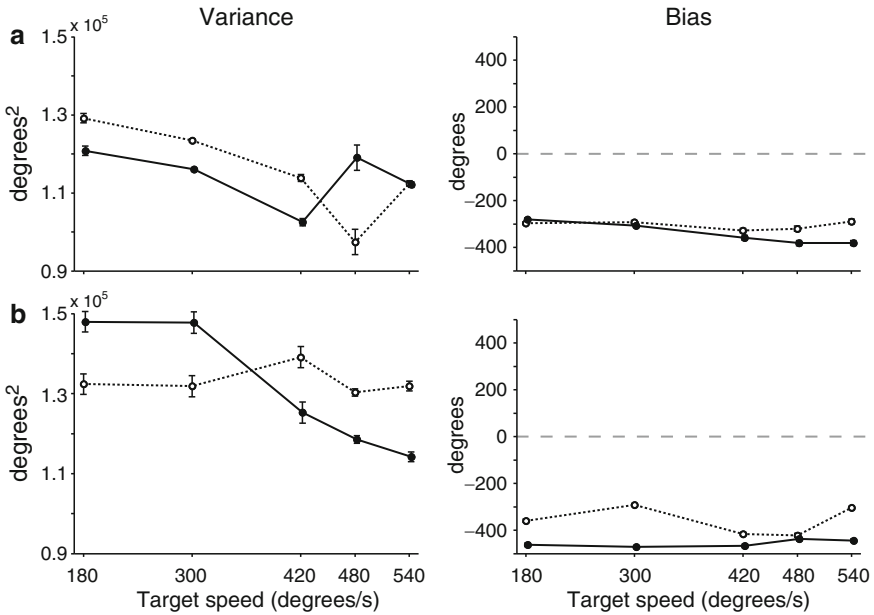
Fig. 6 Mean (±SEM) decodification variance (*left*) and bias (*right*) of the angular position as a function of the target speed. (**a**) Area 7a. (**b**) Motor cortex. *Filled circles* and continuous line correspond to real motion; *open circles* and *dashed line* correspond to apparent motion

The mean decoded angular position over time across target speeds and motion conditions are depicted in Fig. 5 for area 7a and the motor cortex. It is evident that the resulting reconstruction was quite accurate across target speeds and motion conditions in area 7a (Fig. 5a), but deficient in the motor cortex (Fig. 5b). In fact, the mean decoding variability and the mean bias for angular position in both motion conditions were large in the motor cortex (Fig. 6b), but closer to zero in area 7a (Fig. 6a). These results confirm that area 7a is an important node for visual-motion processing [27, 33], and that the neurons in this area can properly represent the change in angular position of the target over time, not only in the real but also in the apparent motion condition [24]. In addition, the results suggest that the motor cortex has limited access to the spatial position of the target during the interception task in both motion conditions. Finally, in accord with the encoding results from the previous section, the decoding from motor cortical activity suggests that the target angle (DTC_{tar}) is probably not the variable used to trigger the interception movement under these conditions.

Figure 7 show the reconstructed TTC_{tar} across target speeds and motion conditions for the motor cortex and area 7a. Again, area 7a (Fig. 7a) shows a decoded TTC that is close to the actual TTC_{tar} for every target speed of the real and apparent
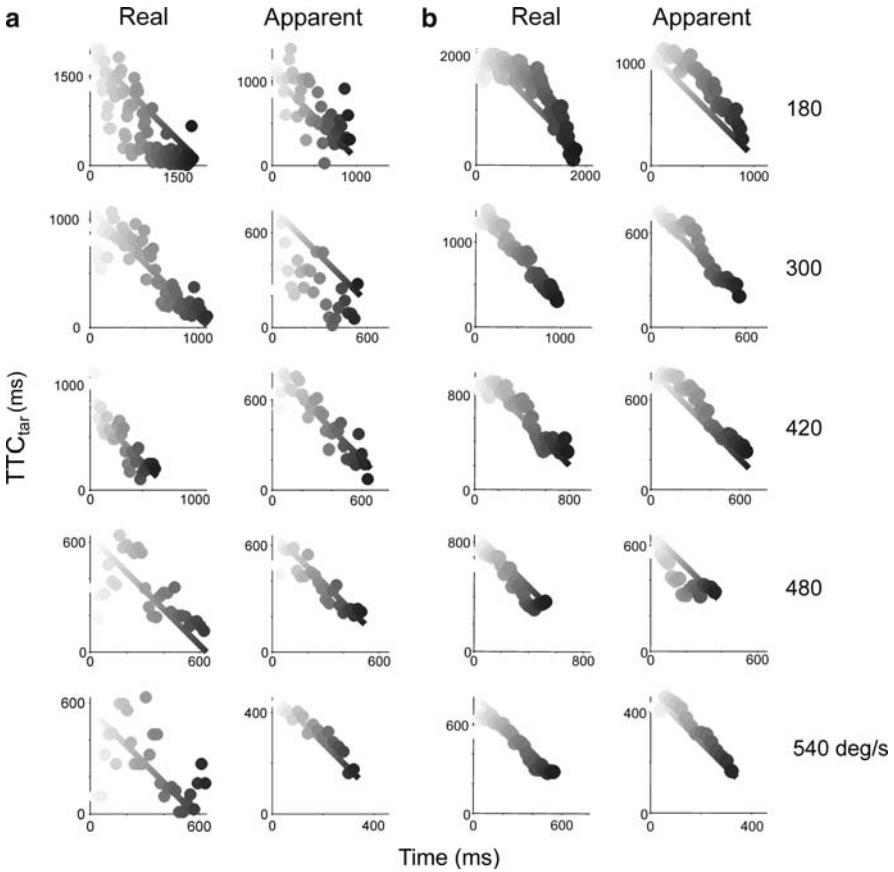
Fig. 7 Mean predicted TTC_{tar} using ensembles of 50 neurons during the real and apparent motion conditions and for the five different stimulus speeds. (**a**) Area 7a. (**b**) Motor cortex. Same notation as in Fig. 5

motion. In addition, the motor cortex (Fig. 7b) shows also an accurate TTC_{tar} decodification during both motion conditions. Actually, the mean decoding variability and mean bias for the target TTC was close to zero in the real and apparent motion conditions using populations of motor cortical (Fig. 8b) or area 7a (Fig. 8a) cells, particularly for the highest speeds. These results indicate, first, that the motor cortex had access to an accurate representation of TTC_{tar} information. This temporal information is probably coming from premotor and posterior parietal areas. Second, these results strengthen the evidence for the hypothesis that TTC_{tar} is the critical target parameter used to trigger the interception movement in this particular task.
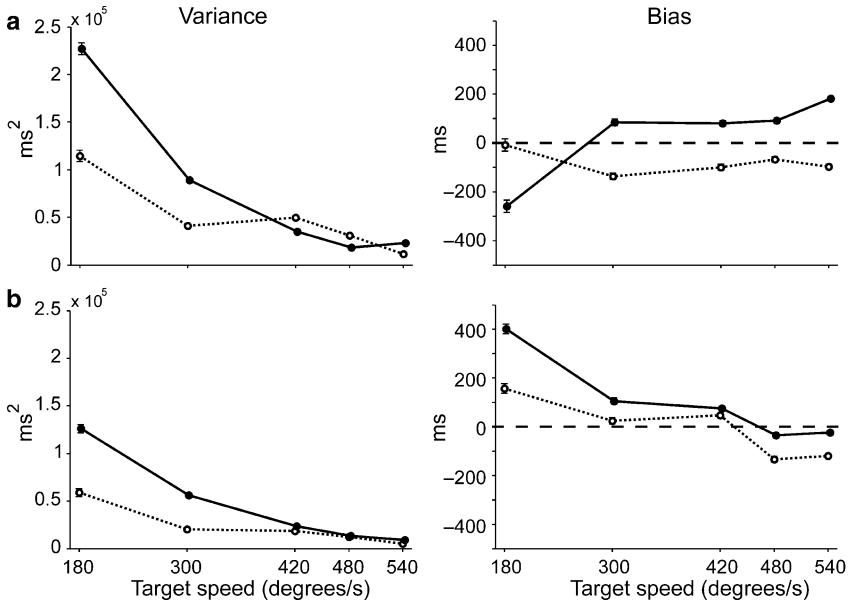
Fig. 8 Mean (±SEM) decodification variance (*left*) and bias (*right*) of the TTC$_{tar}$ as a function of the target speed. (**a**) Area 7a. (**b**) Motor cortex. Filled circles and continuous line correspond to real motion; open circles and dashed line correspond to apparent motion

Concluding Remarks

The neurophysiological experiments using our target interception task revealed that the parietofrontal system of primates is engaged in the representation of spatial and temporal parameters of the target motion. Area 7a processed the target angle and TTC as a sensory area, with a clear preference for the spatial parameter. These findings not only emphasize the role of area 7a in visual motion processing, but also suggest that the representation of TTC begins in the parietal lobe. Actually, imaging and neurophysiological studies have demonstrated that the PPC is involved in temporal information processing [16, 31].

A larger population of motor cortical cells encoded TTC$_{tar}$ than target angle. This information was represented in a predictive rather than a sensory fashion. In addition, the estimated TTC using the activity of motor cortical cells was more accurate than the angular trajectory of the target. Therefore, it is feasible that the motor system uses this type of temporal information to trigger the interception movement in both motion conditions. In fact, we suggest that the motor cortex has the ability not only to represent in a predictive way the TTC$_{tar}$, but also to detect when it reaches a specific magnitude in order to trigger the interception movement.

Our initial observations using a multiple linear regression model suggested that in the real motion condition the angular position of the target was the critical interception variable, whereas in the apparent motion condition it was the TTC. The

current encoding and decoding results indicate that the nervous system represents spatial and temporal parameters of the moving target in the parietofrontal circuit. However, the present findings also suggest that in both the real and apparent motion conditions, the motor system may use the TTC to control the initiation of the interception movement. Since the present encoding models are more specific and were supported by the decoding results, it is more likely that the key interception parameter was temporal rather than spatial in both motion conditions.

Taken together, these results indicate that neurons in the motor cortex and area 7a are processing different target parameters during the interception task. However, the predictive representation of the target TTC is the most probable variable used in the motor cortex to trigger the interception movement.

References

1. Andersen RA. Neural mechanisms of visual motion perception in primates. *Neuron* 18: 865–872, 1997.
2. Battaglia-Mayer A, Ferraina S, Genovesio A, Marconi B, Squatrito S, Molinari M, Lacquaniti F, Caminiti R. Eye-hand coordination during reaching. II. An analysis of the relationships between visuomanual signals in parietal cortex and parieto-frontal association projections. *Cereb Cortex* 11: 528–544, 2001.
3. Bradley DC, Maxwell M, Andersen RA, Banks MS, Shenoy KV. Neural mechanisms of heading perception in primate visual cortex. *Science* 273: 1544–1547, 1996.
4. Bruce C, Desimone R, Gross CG. Visual properties of neurons in a polysensory area in superior temporal sulcus of the macaque. *J Neurophysiol* 46: 369–384, 1981.
5. Cheng K, Fujita H, Kanno I, Miura S, Tanaka K. Human cortical regions activated by wide-field visual motion: an H2(15)O PET study. *J Neurophysiol* 74: 413–427, 1995.
6. Colby CL, Duhamel JR, Goldberg ME. Ventral intraparietal area of the macaque: anatomic location and visual response properties. *J Neurophysiol* 69: 902–914, 1993.
7. Dayan P, Abbott LF. Theoretical Neuroscience, computational and mathematical modeling of neural systems. MIT press. London England, 2001.
8. Donkelaar P van, Lee RG, Gellman RS. Control strategies in directing the hand to moving targets. *Exp Brain Res* 91: 151–161, 1992.
9. Duffy CJ, Wurtz RH. Sensitivity of MST neurons to optic flow stimuli. I. A continuum of response selectivity to large-field stimuli. *J Neurophysiol* 65: 1329–1345, 1991.
10. Duffy CJ, Wurtz RH. Response of monkey MST neurons to optic flow stimuli with shifted centers of motion. *J Neurosci* 15: 5192–5208, 1995.
11. Duffy CJ, Wurtz RH. Medial superior temporal area neurons respond to speed patterns of optic flow. *J Neurosci* 17: 2839–2851, 1997.
12. Field DT, Wann JP. Perceiving time to collision activates the sensorimotor cortex. *Curr Biol* 15: 453–458, 2005.
13. Georgopoulos AP. Neural aspects of cognitive motor control. *Curr Opin Neurobiol* 10: 238–241, 2000.
14. Lee DN, Reddish PE. Plummeting gannets: a paradigm of ecological optics. *Nature* 293: 293–294, 1981.

15. Lee DN. Guiding movement by coupling taus. *Ecological Psychol* 10: 221–250, 1998.

16. Leon MI, Shadlen MN. Representation of time by neurons in the posterior parietal cortex of the macaque. *Neuron* 38: 317–327, 2003.

17. Maunsell JH, Van Essen DC. Functional properties of neurons in middle temporal visual area of the macaque monkey. I. Selectivity for stimulus direction, speed, and orientation. *J Neurophysiol.* 49:1127–1147, 1983.

18. Merchant H, Battaglia-Mayer A, Georgopoulos AP. Effects of optic flow in motor cortex area 7a. *J Neurophysiol* 86: 1937–1954, 2001.

19. Merchant H, Battaglia-Mayer A, Georgopoulos, AP. Functional organization of parietal neuronal responses to optic flow stimuli. *J Neurophysiol* 90: 675–682, 2003a.

20. Merchant H, Battaglia-Mayer A, Georgopoulos, AP. Interception of real and apparent circularly moving targets: Psychophysics in Human Subjects and Monkeys. *Exp Brain Res* 152: 106–112, 2003b.

21. Merchant H, Battaglia-Mayer A, Georgopoulos, AP. Neural responses in motor cortex and area 7a to real and apparent motion. *Exp Brain Res* 154: 291–307, 2004a.

22. Merchant H, Battaglia-Mayer A, Georgopoulos, AP. Neural responses during interception of real and apparent circularly moving targets in motor cortex and area 7a. *Cereb Cortex* 14: 314–331, 2004b.

23. Merchant H, Battaglia-Mayer A, Georgopoulos, AP. Neurophysiology of the parieto-frontal system during target interception. *Neurol. Clin Neurophysiol* 1: 1–5, 2004c.

24. Merchant H, Battaglia-Mayer A, Georgopoulos, AP. Decoding of path-guided apparent motion from neural ensembles in posterior parietal cortex. *Exp Brain Res* 161: 532–540, 2005.

25. Merchant H, Georgopoulos AP. Neurophysiology of perceptual and motor aspects of interception. *J Neurophysiol* 95: 1–13, 2006.

26. Merchant H, Zarco W, Prado L, Perez O. Behavioral and neurophysiological aspects of target interception. *Adv Exp Med Biol* 629: 199–218, 2008.

27. Motter BC, Mountcastle VB. The functional properties of the light-sensitive neurons of the posterior parietal cortex studied in waking monkeys: Foveal sparing and opponent vector organization. *J Neurosci* 1: 3–26, 1981.

28. Newsome WT, Britten KH, Salzman CD, Movshon JA. Neuronal mechanisms of motion perception. *Cold Spring Harb Symp Quant Biol* 55: 697–705, 1990.

29. Phinney RE, Siegel RM. Speed selectivity for optic flow in area 7a of the behaving monkey. *Cereb Cortex* 10: 413–421, 2000.

30. Port NL, Kruse W, Lee D, Georgopoulos AP. Motor cortical activity during interception of moving targets. *J Cogn Neurosci* 13: 306–318, 2001.

31. Rao SM, Mayer AR, Harrington DL. The evolution of brain activation during temporal processing. *Nat Neurosci* 4(3): 317–323, 2001.

32. Shepard RN, Zare SL. Path-guided apparent motion. *Science* 220: 632–634, 1983.

33. Siegel RM, Read HL. Analysis of optic flow in the monkey parietal area 7a. *Cereb Cortex* 7: 327–346, 1997.

34. Tresilian JR. Hitting a moving target: Perception and action in the timing of rapid interceptions. *Percept Psychophys* 67: 129–149, 2005.

35. Van Essen DC, Maunsell JH, Bixby JL. The middle temporal visual area in the macaque: Myeloarchitecture, connections, functional properties and topographic organization. *J Comp Neurol* 199: 293–326, 1981.

36. Wise SP, Boussaoud D, Johnson PB, Caminiti R. Premotor and parietal cortex: corticocortical connectivity and combinatorial computations. *Annu Rev Neurosci* 20: 25–42, 1997.

37. Zeki, SM. Functional organization of a visual area in the posterior bank of the superior temporal sulcus of the rhesus monkey. *J Physiol* 236: 549–573, 1974.

38. Zeki S, Watson JD, Lueck CJ, Friston KJ, Kennard C, Frackowiak RS. A direct demonstration of functional specialization in human visual cortex. *J Neurosci* 11: 641–649, 1991.